




## Article

# Mechanical Performance of Date-Palm-Fiber-Reinforced Concrete Containing Silica Fume

Yasser E. Ibrahim <sup>1,\*</sup>, Musa Adamu <sup>1,\*</sup>, Mohammad Louay Marouf <sup>1</sup>, Omar Shabbir Ahmed <sup>1</sup>, Q. A. Drmosh <sup>2</sup> and Mohammad Abdul Malik <sup>1</sup>

<sup>1</sup> Engineering Management Department, College of Engineering, Prince Sultan University, Riyadh 11586, Saudi Arabia

<sup>2</sup> Interdisciplinary Research Center for Hydrogen and Energy Storage, King Fahd University of Petroleum and Minerals, Dhahran 31216, Saudi Arabia

\* Correspondence: ymansour@psu.edu.sa (Y.E.I.); madamu@psu.edu.sa (M.A.)

**Abstract:** The use of date palm fiber (DPF) as natural fiber in concrete and mortar continues to gain acceptability due to its low-cost and availability. However, the main disadvantage of DPF in cement-based composites is that it reduces compressive strength and increases the porosity of the composite. Hence, for DPF to be efficiently used in concrete, its negative effects must be counteracted. Therefore, in this study, silica fume was employed as supplementary cementitious material to alleviate the negative effects of DPF on the strength and porosity of concrete. The DPF was added in different dosages of 0%, 1%, 2%, and 3% by weight of binder materials. Silica fume was used as a cement replacement material at dosages of 0% to 15% (intervals of 5%) by volume of cement. The unit weights, mechanical strengths, water absorption, and microstructural morphology were all evaluated. The concrete's fresh and hardened densities were reduced with the increment in DPF and silica fume. The compressive strength declined at all ages with the increment in DPF addition, while the flexural and splitting tensile strengths improved with addition of up to 2% DPF. Furthermore, the concrete's water absorption escalated with an increase in DPF content. Silica fume significantly enhanced the mechanical strength of the concrete. The dissipation in compressive strength with the addition of up to 2% DPF was mitigated by replacing up to 10% cement with silica fume, where it densified the microstructure and refined the interfacial transition zone between the fibers and cement matrix, hence significantly decreasing the porosity and enhancing durability.

**Keywords:** natural fiber; date palm fiber; silica fume; composites; date-palm-fiber-reinforced concrete; mechanical properties



**Citation:** Ibrahim, Y.E.; Adamu, M.; Marouf, M.L.; Ahmed, O.S.; Drmosh, Q.A.; Malik, M.A. Mechanical Performance of Date-Palm-Fiber-Reinforced Concrete Containing Silica Fume. *Buildings* **2022**, *12*, 1642. <https://doi.org/10.3390/buildings12101642>

Academic Editor: Tomáš Dvorský

Received: 22 September 2022

Accepted: 7 October 2022

Published: 10 October 2022

**Publisher's Note:** MDPI stays neutral with regard to jurisdictional claims in published maps and institutional affiliations.



**Copyright:** © 2022 by the authors. Licensee MDPI, Basel, Switzerland. This article is an open access article distributed under the terms and conditions of the Creative Commons Attribution (CC BY) license (<https://creativecommons.org/licenses/by/4.0/>).

## 1. Introduction

The use of sustainable construction and building materials offers a series of advantages, such as lower production and maintenance cost, environmental friendliness, biodegradability, non-toxicity, and improved mechanical performance [1]. Concrete has been the most utilized building and construction material because of its series of advantages, such as high strength and durability, good quality, lower strength-to-cost ratio, and ability to be easily cast into various shapes compared to other construction materials such as steel and timber [2,3]. However, concrete's high brittleness, poor tensile strength, low strain, and low bending resistance are its main drawbacks. Due to this, concrete is prone to cracking while under tensile loads. To overcome these concrete shortcomings, reinforcement is normally used with concrete to form a composite action i.e., reinforced concrete elements. However, due to the high cost of reinforcement, fibers are incorporated in concrete to enhance its tensile strength and minimize the amount of reinforcement required to achieve tensile strength. Additionally, fibers are used in plain concrete to enhance its tensile strength. Reinforcing fibers of various kinds, classified as either natural or synthetic, have been

employed in concrete to enhance its hardened and physical qualities. [4–6]. Glass, steel, organic plastics, and polymers are the best reinforcing materials used in concrete. A few naturally occurring fibers, such as asbestos and cellulose, as well as agricultural fibers such as jute, sisal, date palm mesh, etc., are also utilized in concrete [7,8]. DPF is one of the popular, inexpensive, environmentally beneficial, and sustainable natural fibers. The date palm tree produces vast amounts of waste, much of which is discarded without being properly utilized. Comparing DPF to other natural and synthetic fibers, it has the distinct benefit of having a higher strength-to-cost ratio [9].

Several studies have reported that DPF has been used as natural fiber in cement-based materials such as concrete and mortar. Ozerkan, Ahsan [10] added DPF in dosages of 0%, 0.5%, 1%, and 2% in mortar. The initial and final settings times and drying shrinkage of the mortar increased with the addition of up to 1% DPF and declined with the addition of 2% fiber. Furthermore, DPF escalated the rate of water absorption of the mortar, with 0.5% addition being the optimum. They also reported improvement in mechanical properties and sulfate attack resistance with the addition of up to 1% DPF, which they attributed to better compaction between the fibers and cement matrix resulting in good homogeneity in the mix. Benaniba, Driss [11] developed a DPF–cement mortar composite using different proportions of DPF (6% to 30% at intervals of 6%) by weight. They reported a significant increase in water absorption, and a decrease in density, thermal conductivity, flexural and compressive strengths with the increment in the percentage of DPF. There was an improvement in the flexural strength at a lower dosage of 6% and 12% compared to plain cement mortar. In a related work, Zanichelli, Carpinteri [12] evaluated the fracture behavior of mortar reinforced with DPF at different proportions from 2% to 10% (at intervals of 2%) by volume. They reported a reduction in peak load, elastic modulus, and fracture toughness with an increment in DPF addition. On the contrary, their results showed improved ductile behavior and energy absorption with the increment in DPF content. Based on their findings, they recommended using DPF-reinforced mortar for nonstructural applications where high strength is not important and structures where lightweight and durability are very significant. Vantadori, Carpinteri [1] examined the impact of DPF in cement mortar, where they added DPF in varying proportions from 2% to 10% (interval of 2%) by volume. They observed a decline in density, flexural strength, and fracture toughness with the increment in fiber content. There was a reduction between 9–52% and 7–66% for the modulus of rupture and fracture toughness, respectively, with the addition of 2–10% DPF. The ductility and energy absorption capacity of the mortar enhanced with percentage increase in DPF, where an increase between 27–162% was found with addition of 2–10% DPF compared to the plain mortar. Kareche, Agoudjil [13] investigated DPF's impact on the durability performance of cement mortar, where they incorporated DPF at different proportions of 5%, 10%, and 15% by weight. They reported a surge in porosity and a decline in drying shrinkage in the mortar with DPF addition. The addition of 15% DPF led to an increment in porosity by up to 51% and a decline in drying shrinkage up to 71.4%. Additionally, they reported an improvement in the acid attack resistance (sulfuric attack), and a reduction in the compressive strength and resistance to cyclic wetting and drying with the increment in DPF content. Alatshan, Altomate [14] prepared several mixes by addition different DPF dosages of 0.5%, 1%, 1.5%, 2% and 2.5% for fiber lengths of 50 mm, 60 mm, and 70 mm. They noticed a reduction in the compressive strength due the high content of DPF dosage and length. However, the concrete's compressive strength reinforced with 0.5%–50 mm DPF was reported to be of a higher strength than plain concrete due to the tensile strength of the added DPF. The flexural strength was moderately enhanced with a lower dosage of DPF of all lengths. The flexural strength of composites with 0.5%–50 mm DPF, 1%–60 mm DPF, and 0.5%–70 mm DPF were higher in comparison to the conventional concrete due to the tensile strength of the fiber. However, for all other dosages and fiber length mix combinations, there was depletion in the flexural strength.

Based on the available studies, concrete and mortar reinforced with DPF have several advantages compared to plain concrete and mortar, which include lower density,

lightweight, higher ductility and energy absorption capacity, lower thermal conductivity, higher thermal insulation, and resistivity. These properties improve thermal comfortability and energy savings in buildings through good thermal insulation [15,16]. However, the major challenge and disadvantage of using DPF in concrete and mortar is the reduction in mechanical properties and elastic modulus [17–19]. Additionally, DPF affects the durability performance of cementitious composites through increased water absorption, porosity, drying shrinkage, etc. These negative effects are caused mainly by the increase in pore volume in the composite's microstructure, poor adhesion between fibers and cement paste, and the hydrophilic nature of the DPF, making it absorb more water and swell during mixing [16]. Therefore, for DPF to be effectively added in concrete and mortar to derive its maximum benefits, methods for reducing or mitigating its undesirable effect on the cement composite's performance must be derived. Several studies treated DPF using different methods; some methods were slightly effective, while others further caused reduction in the mechanical properties. SCM such as nano silica and silica fume has been used in fiber-reinforced concrete to overcome the fiber's negative effects on the composite's performance. Gencel, Nodehi [20] used silica fume as an SCM in basalt-fiber-reinforced foam concrete (BFRFC). They added basalt fiber in three volumes, i.e., 0%, 1.5%, and 3%, and partially substituted cement with silica fume at 0% and 15%. They reported a decrease in the workability (flowability) and density of the concrete with silica fume addition, where a decrease by 16% was observed with 15% silica fume addition. They reported an increased in thermal conductivity, elastic modulus, flexural, and compressive strengths for the BFRFC with the inclusion of silica fume. The addition of 15% silica fume to the BFRFC containing 0%, 1.5%, and 3% improved the 28 days compressive strength by 54%, 70.5%, and 66.8%, respectively, and the 28 days flexural strength by 5.8%, 9.4%, and 8.9%, respectively. Furthermore, they reported a decrease in the porosity, water absorption, and splitting tensile strength of the BFRFC with silica fume addition. For 15% silica fume addition to the BFRFC containing 0%, 1.5%, and 3% fiber, the porosity decreased by 51.2%, 23.2%, and 35.2%, respectively, the water absorption decreased by 52.2%, 24.4%, and 35.7%, respectively, and the tensile strength diminished by 16.7%, 12.5%, and 4.6%, respectively. Sadrumontazi, Tahmouresi [21] examined the effects of silica fume as a SCM on basalt-fiber-reinforced cementitious composite (BFRCC)'s properties. They prepared several mixes by adding basalt fiber at different proportions by volume (0%, 1%, and 1.5%) and substituted cement using silica fume at different percentages by weight (5%, 10%, and 15%). The increment in silica fume reduced the workability, where a 15% silica fume addition decreased the flowability of the BFRCC by 28%, 19%, and 21% for 0%, 1%, and 1.5% fiber content, respectively, while the flexural and compressive strengths of the BFRCC were enhanced with the inclusion of silica fume for any fiber content. For a 5% silica fume addition, there was enhancement in compressive strength by 23%, 37%, and 12%, and flexural strength by 4%, 12%, and 5% for BFRCC containing 0%, 1%, and 1.5% fiber, respectively. Khan, Rehman [22] utilized silica fume as an SCM in coconut-fiber-reinforced concrete (CFRC). They prepared the CFRC by adding 2% by weight coconut fiber and replaced cement with different proportions of silica fume between 5–20%. The modulus of rupture, splitting tensile, and compressive strengths of the CFRC improved substantially with the increment in silica fume content. Replacement of cement with 5%, 10%, 15%, and 20% in the CFRC resulted in an increase in compressive strength by 5.8%, 10.8%, 24.6%, and 3%, respectively, and the modulus of elasticity by 10.8%, 22%, 33.6%, and 1.2%, respectively. The splitting tensile strength increased by 25.9%, 29.6%, and 33.5%, while the flexural strength increased by 26.9%, 50%, and 59.6% for 5%, 10%, and 15% silica fume addition to the CFRC, respectively, when compared to plain concrete.

Other materials have been used to improve the performance of both plain and fiber-reinforced concrete. Zhang, Wang [23] added nano silica to improve the performance of fly ash (30%) and metakaolin (70%)-based polyvinyl-alcohol (PVA)-fiber-reinforced geopolymer/alkali-activated mortar. They added PVA fiber at, 0.2%, 0.4%, 0.6%, 0.8%, 1.0%, and 1.2% by volume of mortar and 1% nano silica by weight of binder. They reported a

reduction in slump of 26.4% with the addition of 0 to 1.2% PVA, while 1% nano silica slightly increased the slump. The compressive strength, flexural strength, and elastic modulus of the mortar increased with the addition of nano silica and PVA fiber. The 1% nano silica increased the strength by up to 29.1%, while up to 0.8% PVA increased the strength by 27.6%. They achieved the highest strength with addition of 1% nano silica and 0.8% PVA. Up to a 68% increase in flexural strength was reported with addition of PVA. The elastic modulus increased by 20–130% with addition of 0.2% to 1.2% PVA. Furthermore, the addition of up to 1% PVA enhanced the fracture toughness of the mortar, and nano silica also enhanced the load-carrying capacity of the mortar with up to 0.6% PVA. Golewski [24] studied the effects of different SCMs on the properties of concrete. They used fly ash, silica fume, and nano silica as the SCM. They replaced cement with a constant dosage of silica fume and nano silica at 10% and 5%, respectively, while for fly ash they used different replacement proportions of 0%, 5%, and 15%. When compared to the plain concrete, all the quaternary blend concretes demonstrated a higher strength. For the blended concrete, they reported a reduction in compressive strength with the increment in fly ash content. The quaternary blend with 5% fly ash, 10% silica fume, and 5% nano silica gave the best strength and fracture toughness [25]. In a similar study, Gil and Golewski [26] investigated the effects of the interaction of silica fume and fly ash as SCMs on the properties of concrete. They produced different blends using combinations of different proportions of fly ash between 0% and 20% and silica fume proportions between 0% and 10%. Their findings showed that the concrete blend containing 10% silica fume with 0% fly ash had the best performance in terms compressive and tensile strengths, water absorption, and water penetration, while the fly ash decreased the compressive and tensile strengths and increased the water absorption and depth of penetration of the concrete.

Different types of natural fibers have been used to improve the performance of cementitious composites. However, there are few studies that have utilized DPF as a natural fiber in cementitious composites. The available studies that used DPF mostly used it in mortar, hence there is need for more and also comprehensive studies on the use of DPF in concrete. This is due to the aforementioned advantages of DPF. Based on the available studies, the use to silica fume has proven to significantly enhance the properties of fiber-reinforced concrete. To the best of the authors knowledge, there are limited studies that have investigated the effects of DPF addition and silica fume as a partial replacement for cement to improve the mechanical performance and mitigate the negative effects of the fiber on the strength of the concrete. Hence, in this study, DPF was treated using alkaline solution (NaOH), and silica fume was used as an SCM in the concrete to reduce the porosity and mitigate the undesirable effects of the DPF on the concrete's performance. The DPF was added at different dosages of 1%, 2%, and 3% by weight of binder materials, and silica fume was used to partially replace cement at 5%, 10%, and 15%. The effects of the DPF and silica fume on the fresh, mechanical, and durability performance of the DPF-reinforced concrete was then investigated.

## 2. Materials and Methods

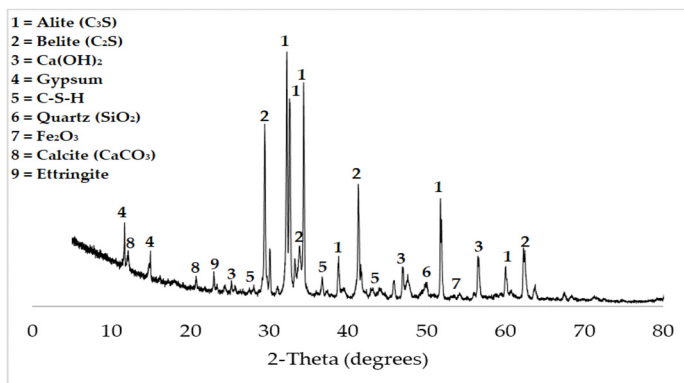
### 2.1. Materials

Type I OPC was used as the main binder material. The properties of the cement conformed to the standard guidelines outlined in ASTM C150/150M [27] and are presented in Table 1, and its X-ray diffraction (XRD) is shown in Figure 1a. Densified silica fume was used as an SCM. The silica fume was obtained from Xiamen All Carbon Company, Xiamen China, through Al-Rashad Cement Company, Saudi Arabia. The silica fume had a specific gravity (SG) of 2.25, bulk density of 630 kg/m<sup>3</sup>, and a specific surface area of 18,000 m<sup>2</sup>/kg. The chemical properties and XRD pattern of the silica fume are presented in Table 1 in Figure 1b, respectively. Natural sand was used as fine aggregate. The properties of the aggregates were in line with ASTM C33 [28] specifications. The fine aggregate was well-graded, with a particle size distribution falling within the limits specified by ASTM C33 [28] as highlighted in Figure 2. Additionally, the fine aggregate had an SG value of

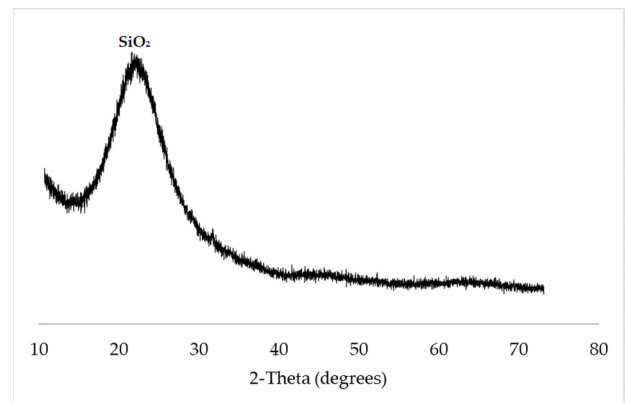
2.63, 1.87% water absorption, 1565 kg/m<sup>3</sup> bulk density, fineness modulus of 2.26, and mud content of 1.1%. The coarse aggregate utilized was crushed gravel of 19 mm size, which was well-graded. As demonstrated in Figure 3, the coarse aggregate's particle size distribution also complied with ASTM C33 [28] guidelines. The coarse aggregate had an SG, bulk density, and water absorption of 2.67, 1455 kg/m<sup>3</sup>, and 0.65%, respectively. A polycarboxylate-based water-reducing admixture with a density of 1.060 g/cm<sup>3</sup> was used as a superplasticizer so as to reduce the required quantity of mixing water.

**Table 1.** Properties of binder materials.

Oxide Composition (%)	Cement	Silica Fume
CaO	65.18	0.21
Al <sub>2</sub> O <sub>3</sub>	5.39	0.26
Fe <sub>2</sub> O <sub>3</sub>	3.40	0.05
SiO <sub>2</sub>	19.71	95.85
MgO	0.91	0.45
Na <sub>2</sub> O	0.17	—
K <sub>2</sub> O	1.22	—
TiO <sub>2</sub>	0.24	—
SO <sub>3</sub>	3.51	1.00
P <sub>2</sub> O <sub>5</sub>	0.09	—
MnO	0.18	—
LOI	2.38	2.80



(a) Cement



(b) Silica fume

**Figure 1.** XRD pattern of binder materials.

The DPF used in this study was obtained from the Aldebass farm in Majmaah, Saudi Arabia. The fiber was plucked from the trunks of date palm trees in the form of a natural rectangular woven mesh in three superposing layers and was about 200–300 mm in width and 300–500 mm in length as shown in Figure 4a. Before treatment, the fiber was immersed in water, separated into single fibers of about 0.2–1.0 mm diameter, and cut to a fiber length of 20–30 mm. The DPF was then treated using alkaline solution, i.e., a 3% NaOH solution for 3 h based on the recommendation of Ali-Boucetta, Ayat [29]. After treatment, the DPF was then thoroughly washed with clean water and air dried for 48 h before use in the concrete. Figure 4b shows the processed DPF ready to be used. Table 2 presents the physical and mechanical properties of the DPF.

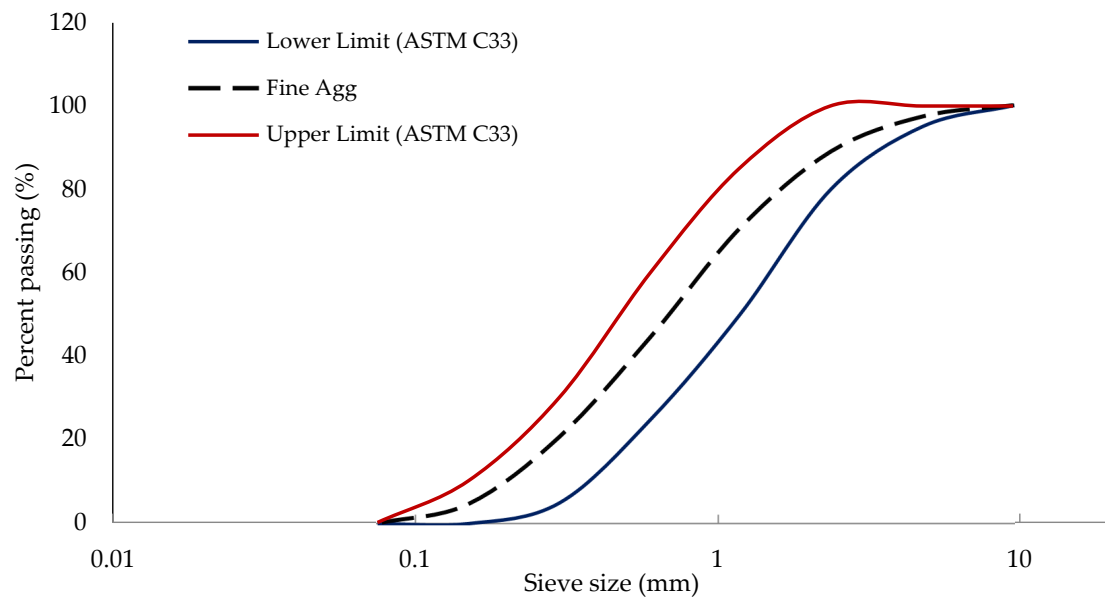


**Figure 2.** Fine aggregate gradation.

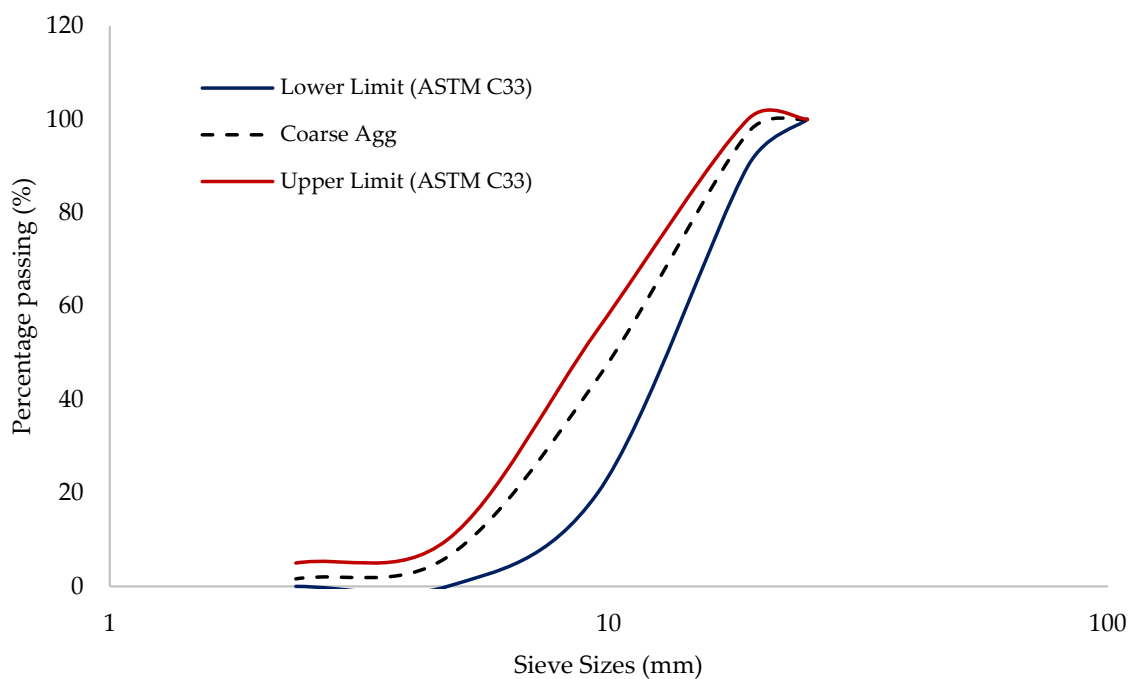


**Figure 3.** Coarse aggregate gradation.

**Table 2.** Properties of DPF (1).

Property	Value
Diameter (mm)	0.2–1.0
Length (mm)	20–30
Bulk density (kg/m <sup>3</sup> )	877.43 ± 4.8
Natural moisture content (%)	10.2 ± 0.4
Water absorption to saturation (%)	102.65 ± 3.3
Tensile strength (MPa)	203.24 ± 30
Elongation at break (%)	13.5 ± 2
Modulus of elasticity (GPa)	3.35 ± 1.5



**Figure 4.** Date palm fiber.

### 2.2. Mix Proportioning

The control concrete mix design was carried out adopting ACI 211.1R [30] based on the absolute volume method. The quantity of superplasticizer used throughout all the mixes was constant (1% by mass of binder) to mitigate the effects of water-to-cementitious materials ratio variations and to cut down the quantity of mixing water needed to obtain a standard consistency. The treated date palm fiber (DPF) was added in variations of 0%, 1%, 2%, and 3% by mass of binder. Silica fume was used as partial replacement to cement using the volume replacement method in different percentages by weight of binder materials at 0%, 5%, 10%, and 15%. A total of thirteen (13) mixes were generated as displayed in Table 3. Each of the mixes was named based on the quantities of the variables. Mix M1F0S was a mix comprising of 1% DPF and 0% silica fume, while mix M2F10S was a mix with 2% DPF and 10% silica fume and mix M3F15S was a mix with 3% DPF and 15% silica fume.

**Table 3.** Properties of DPF (2).

Mix	Variables (%)		Quantities in kg/m <sup>3</sup>						
	Fiber (%)	Silica Fume (%)	Cement	Silica Fume	Fiber	Fine Agg	Coarse Agg	Water	S. P *
Control	0	0	490	0.0	0.0	750	905	185	4.9
M1F0S	1	0	490	0.0	4.9	750	905	185	4.9
M2F0S	2	0	490	0.0	9.8	750	905	185	4.9
M3F0S	3	0	490	0.0	14.7	750	905	185	4.9
M1F5S	1	5	465.5	17.9	4.83	750	905	185	4.8
M2F5S	2	5	465.5	17.9	9.67	750	905	185	4.8
M3F5S	3	5	465.5	17.9	14.50	750	905	185	4.8
M1F10S	1	10	441	35.8	4.77	750	905	185	4.8
M2F10S	2	10	441	35.8	9.54	750	905	185	4.8
M3F10S	3	10	441	35.8	14.30	750	905	185	4.8
M1F15S	1	15	416.5	53.7	4.70	750	905	185	4.7
M2F15S	2	15	416.5	53.7	9.40	750	905	185	4.7
M3F15S	3	15	416.5	53.7	14.11	750	905	185	4.7

\* S.P = Superplasticizer, Agg = Aggregate.

### 2.3. Samples Preparation and Test Methods

The mixing, sampling, and curing of the concrete were carried out based on the standard procedure highlighted in ASTM C192/C192M [21]. The fresh concrete was mixed using a rotating drum concrete mixer in the laboratory as shown in Figure 5a. Prior to mixing, it was ensured that the aggregates were saturated and surface dried. The cement and silica fume were also devoid of any lumps prior to casting. The batching of

the component ingredients was conducted using the weight approach. The water and superplasticizer were first mixed in a container. The mixing process was as follows: Firstly, the fine aggregate, cement, and silica fume were poured into the mixer, and the mixing began for at least 1 min. Then, the fiber, coarse aggregate, and part of the water were poured. Then, the mixing continued. The remaining water was poured gradually while mixing was ongoing. The mixing continued until a consistent mix was accomplished. The samples were then placed in the designed molds based on the testing conducted, and the fresh density was determined. The samples were cast into the recommended molds as shown in Figure 5b. The samples were air-dried for 24 h in the laboratory prior to demolding. Following removal, the hardened concretes were then cured for the recommended period in water, as shown in Figure 5c, before testing.



(a) Mixing



(b) Cast samples



(c) Curing of samples



(d) Compressive strength testing



(e) Splitting tensile strength testing



(f) Flexural strength testing

**Figure 5.** Experimental Set up.



## 2.4. Test Methods

The density of the freshly mixed concrete was determined instantly after mixing following BS-EN 12350-6 [31], while the density of the hardened concrete (unit weight) was determined regarding BS EN 12390-7 [32] using 100 mm cubes. The standard specifications defined in BS EN 12390-3 [33] were adopted for the determination of the compressive strength of the DPF-reinforced concrete using a universal testing machine (UTM). Cube specimens of 10 cm sizes were prepared and tested as shown in Figure 5d. For each mix, nine specimens tested after 3-, 7-, and 28-days curing duration. Three specimens were tested for each mix after each curing period to obtain the standard errors. The procedures outlined in BS EN 12390-6 [25] were utilized for the splitting tensile strength test. A UTM of 300 kN capacity was used for the testing. Cylinder-shaped specimens of 200 mm height and 100 mm diameter were tested after 3-, 7-, and 28-days curing duration as shown in Figure 5e. The flexural strength test was carried out using the beam with third-point load method as outlined in ASTM C78/C78M [34] using 100 mm × 100 mm × 500 mm prisms as shown in Figure 5f. The samples were tested after curing for a period of 7 and 28 days. The durability of the DPF-reinforced concrete was determined using a water absorption test, which was performed by adopting the procedure outlined in ASTM C642 [35]. Cube samples of 100 mm were made and cured for a period of 28 days before testing. To compute the standard error for each test and each mix, three samples were tested per test/mix/curing time.

The microstructure of the DPF concrete was examined with the aid of field emission scanning electron microscope (FESEM). Some mixes were randomly selected to represent both the DPF and silica fume proportions. After curing the samples for 28 days, the small fracture was extruded, dried, and used for the FESEM test. The sample was then cleaned using a high-pressure vacuum to remove any dust and impurities and to dry it completely. Prior to placing the sample in the FESEM machine, the sample was gold-coated with a thin film. Pictures of a high magnification up to 10,000 were taken from the computer screen attached to the machine. The pictures, with the help of energy dispersive spectroscopy (EDS) obtained from the FESEM machine, were used to analyze the morphology of the concrete.

## 3. Results and Discussions

### 3.1. Fresh Density and Unit Weight

The results of the fresh and hardened unit weights are presented in Figures 6 and 7. Adding DPF led to a slight reduction in both the fresh and hardened unit weight. The fresh unit weight of the concrete decreased by about 2.1%, 4%, and 5.9%, with inclusion of 1%, 2%, and 3% DPF, respectively. At the same time, the hardened unit weight decreased by 3.4%, 4.2%, and 5.4% by adding 1%, 2%, and 3% DPF, respectively. This can be illustrated by comparing the unit weight values of M1F0S, M2F0S, and M3F0S with that of the control mix in Figures 6 and 7. Benaniba, Driss [11] also reported a reduction in the unit weight of concrete with increase in addition of DPF. This gives DPF the advantage of being used as a good insulating material in concrete, as they reported that the lower the density of the DPF concrete, the lower its thermal conductivity. The slight reduction in the unit weight due to the addition of DPF was ascribed to the increased volume of voids in the concrete caused by fiber inclusion resulting from its hydrophilic nature and poor adhesion between the DPF and the concrete, thus increasing the porosity and causing the reduction in unit weight [1,36]. However, the decrease in the unit weight is one of the advantages of using DPF in cementitious composites, as higher thermal properties can be achieved with a lower unit weight. The concrete's fresh and hardened unit weights further decreased with the increment in percentage replacement of cement using silica fume as shown in Figures 6 and 7. For instance, comparing the unit weight values of the mixes comprising of 5% and 10% silica fume content with the same dosage of DPF, those with a higher silica fume content had lower fresh and hardened unit weight values. Mixes M1F5S, M2F5S, and M3F5S had higher fresh and hardened unit weights compared to mixes M1F10S, M2F10S, and M2F10S. Furthermore, mixes with 15% silica fume, i.e., M1F15S, M2F15S, and M3F15S,

had the least fresh and hardened unit weights. Gencil, Nodehi [20] reported a slight reduction in the fresh density by about 4% in basalt-fiber-reinforced concrete when 15% cement was replaced with silica fume, while Saradar, Nemati [37] reported a decrease in the hardened density of basalt-fiber-reinforced concrete with the addition of silica fume as partial substitute to cement. The decrease in unit weight with the increment in silica fume can mainly be attributed to the inferior specific gravity of the silica fume compared to that of cement since the volume substitution method was used.

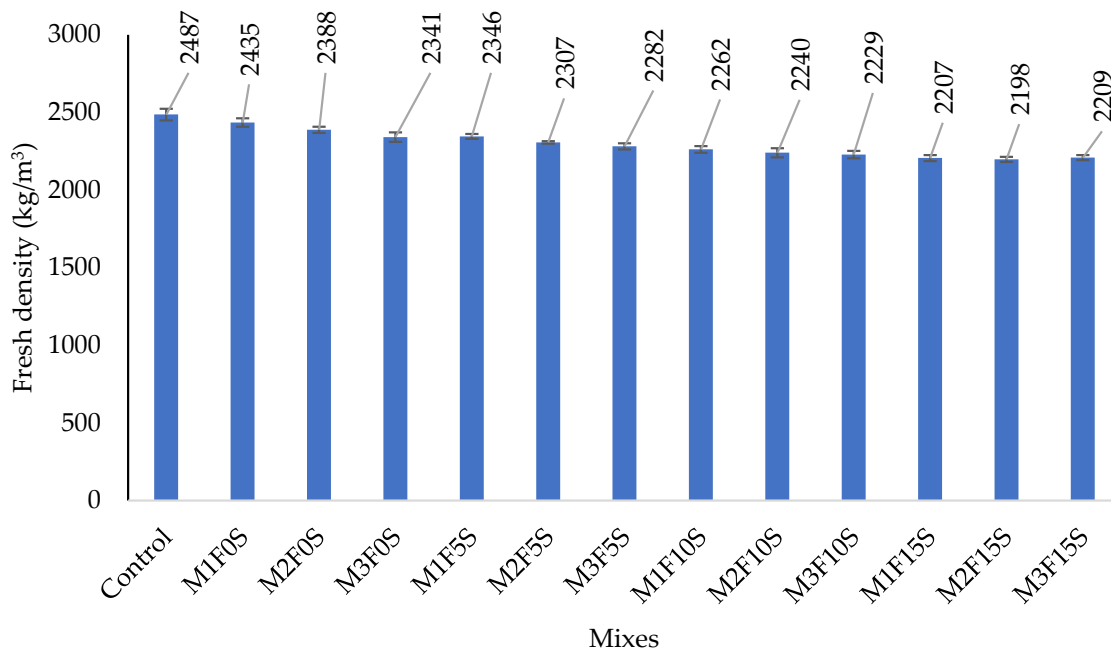


Figure 6. Results of fresh density.

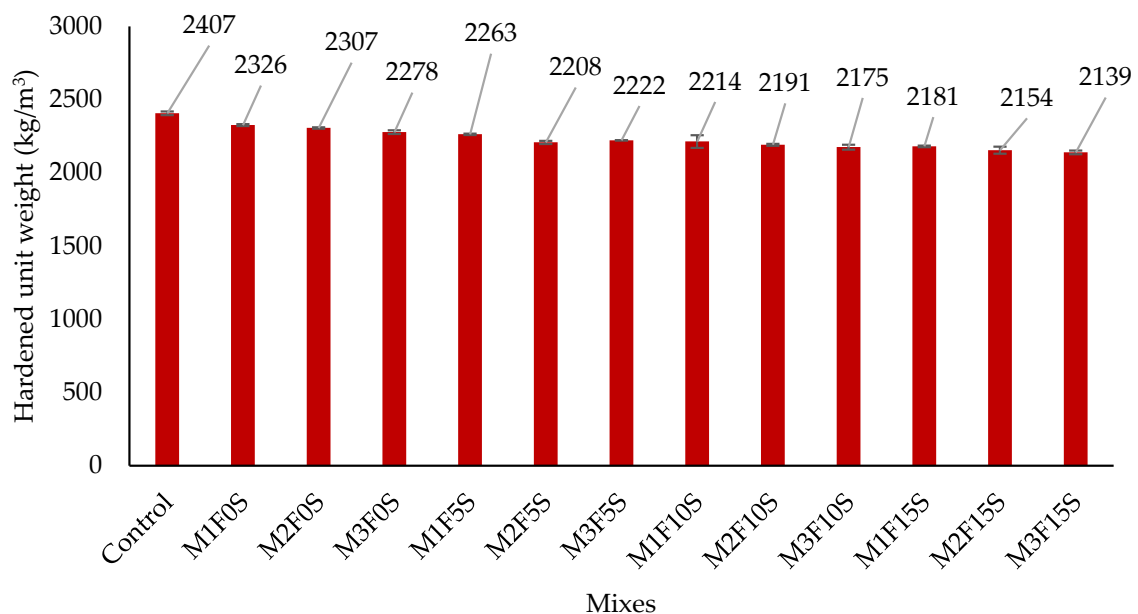


Figure 7. Results of hardened unit weight.

### 3.2. Compressive Strength

The results of the compressive strength of the DPF-reinforced concrete containing different proportions of silica fume as SCM are presented in Figure 8. The compressive strength increased with the curing time due to continuous hydration reactions. The strength

declined with an increment in DPF content at all ages. The 3-day strength declined by 4.03%, 14.2%, and 20.1%, while the 28-day strength decreased by 4.3%, 21.2%, and 20.3% for 1%, 2%, and 3% DPF inclusion, respectively, as seen from mixes M1F0S, M2F0S, and M3F0S in Figure 8. These reductions can be ascribed to the following reasons: (i) the higher porosity in the concrete matrix resulting from air entrained on the fiber surface during mixing, difficult packing and compaction, and a balling effect due to the addition of a high fiber content. (ii) Weak adhesion between the DPF and cementitious paste resulting in a weak interfacial transition zone increasing the weak path for premature failure. (iii) The lower density and strength of the DPF added also affected the density and strength of the concrete [1,38,39]. Additionally, in the presence of the excess cement hydration product, i.e., calcium hydroxide, DPF loses its durability and strength, causing a reduction in the strength of DPF-reinforced concrete [40]. However, the poor bonding between the DPF and cement paste was minimized by treating the DPF with NaOH solution before usage, which eliminated impurities and enhanced the fiber's surface roughness leading to the enhancement of the bondage strength [29]. Benaimche, Carpinteri [41] and Kriker, Debicki [42] also reported a reduction in the strength of concrete with the inclusion of DPF to cementitious composites.

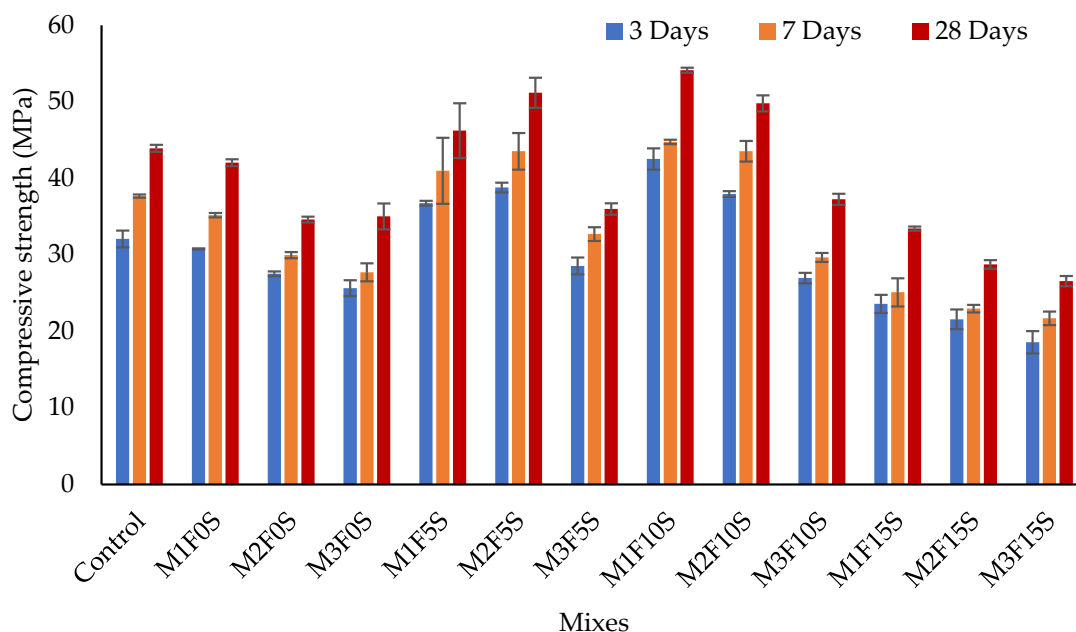


Figure 8. Compressive strength results.

The partial replacement of up to 10% cement with silica fume in the DPF-reinforced concrete enhanced the compressive strength and mitigated the loss in strength due to DPF's undesirable effects. For instance, the compressive strength of mix M1F5S, which contained 5% silica fume as a substitute to cement, was higher than the control mix by 14.6%, 8.8%, and 5.3% at 3, 7 and 28 days, respectively. Likewise, mix M2F5S had a higher compressive strength by 20.9%, 15.5%, and 16.5% at 3, 7 and 28 days, respectively. Similar result improvements were seen for the mixes containing 10% silica fume, i.e., mixes M1F10S and M2F10S at all ages of curing. Therefore, it can be said that the replacement of up to 10% cement using silica fume successfully mitigated the negative effects of up to 2% DPF addition on the compressive strength of the fiber-reinforced concrete. The enhancement in compressive strength with silica fume addition to the DPF concrete resulted from silica fume's higher surface area, thus acting as a filler in addition to it being a pozzolanic material, hence densifying the concrete microstructure and improving the strength. Silica fume contains a very high amount of reactive silica ( $\text{SiO}_2$ ), reacting with cement hydration products such as  $\text{Ca}(\text{OH})_2$  from cement hydration to produce supplementary calcium aluminate silicate hydrate (C-AS-H) and calcium silicate hydrates (C-S-H), which are the major compounds

for strength development in concrete [43,44]. Furthermore, the consumption of the excess calcium hydroxide by the silica fume prevented further deterioration of the durability and strength of the DPF. The improvement in strength was more noticeable at early ages up to 7 days compared to 28 days. This could be because silica fume is a highly reactive SCM, thereby its addition fastens the hydration reaction at early ages [44]. Gencil, Nodehi [20] carried out similar work by using silica fume as an SCM in basalt-fiber-reinforced concrete and found that the compressive strength was enhanced by up to 46% with the replacement of up to 15% cement using silica fume. Saradar, Nemati [37] also reported an increase in compressive strength by about 29% with the replacement of 10% cement with silica fume in basalt-fiber-reinforced concrete containing up to 0.5% fiber. On the contrary, the substitution of cement using a higher silica fume content of 15% reduced the compressive strength. This might have resulted from the fineness of the silica fume, which might have caused it to soak up the mixing water and decrease the consistency. This, in addition to the DPF, resulted to poor compaction, causing porosity in the cement matrix and hence a reduction in strength.

### 3.3. Flexural Strength

The bending resistance of the concrete was measured using a flexural strength test. This is very important, especially when the material will be used to construct flexural members such as beams and slabs. Figure 9 presents the results of the flexural strength of the DPF concrete. The incorporation of DPF resulted in a slight improvement in the flexural strength of the concrete at both 7 and 28 days. The flexural strength increased by about 3%, 9.7%, and 14.8% at 7 days and by 5.3%, 12.8%, and 17.3% at 28 days by incorporating 1%, 2%, and 3% DPF, respectively. As the DPF was treated using NaOH solution, this increased the DPF's surface roughness and improved the bonding between the cement matrix and fiber [29]. In addition to the fiber's bridging effect, this led to a delaying of the crack formation propagation, improving the post-cracking load resistance, hence enhancing the flexural strength. Similar improvements in flexural strength have been reported by Benaniba, Driss [11] with the addition of up to 6% DPF in mortar, and Ali-Boucetta, Ayat [29] with the addition of 2% DPF, and [10] found an improvement in flexural strength with the addition of up to 1% DPF to cement mortar.

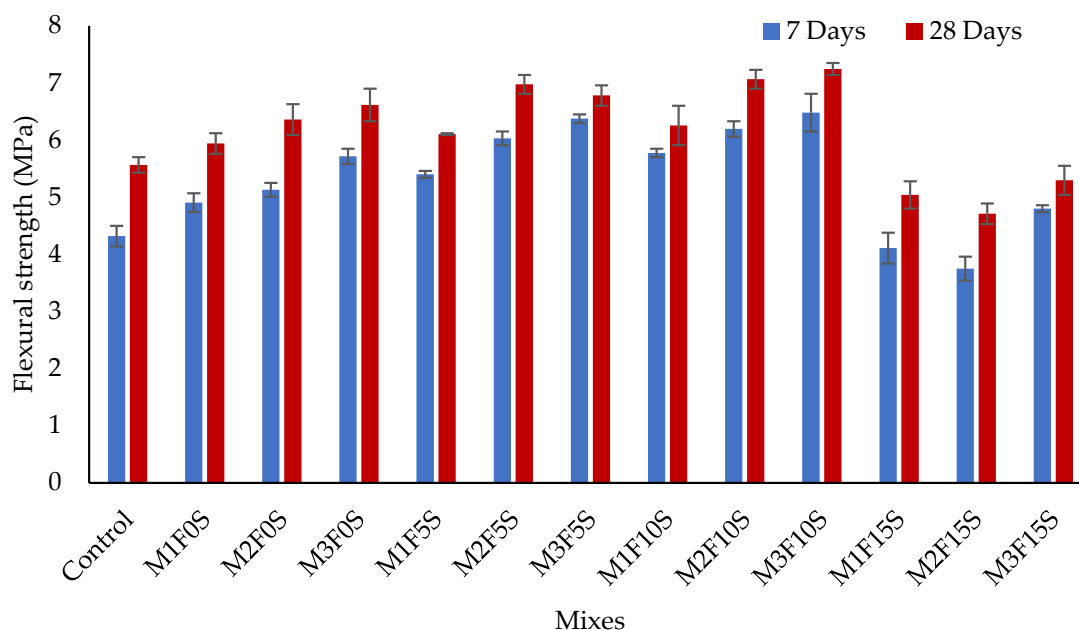


Figure 9. Flexural strength results.

Partially substituting up to 10% cement with silica fume enhanced the flexural strength of the DPF-reinforced concrete at both 7 and 28 days. This is further explained by comparing

the flexural strength values of the mixes containing 5% and 10% silica fume with those without any silica fume addition with the same amount of DPF. For the mixes containing 1% DPF at 7 days, the flexural strength of the mixes M1F5S and M1F10S were greater by 16.3% and 25.4 %, respectively, and at 28 days by 5.81% and 7.83%, respectively, compared to mix M1F0S. Similar results were seen for the mixes containing 2% DPF and 3% DPF, as shown in Figure 9. This clearly explains the synergetic effects of DPF and silica fume. The enhancement in the bending resistance of the DPF-reinforced concrete with the addition of silica fume can be attributed to the high pozzolanic-hydration reactivity between the silica fume compounds, i.e.,  $\text{SiO}_2$  and cement hydration by-products, i.e.,  $\text{Ca}(\text{OH})_2$ , to produce surplus hydration compounds, which filled the pores created by the DPF and densified the concrete microstructure. This resulted in the improved adhesion and densification of the ITZ between the cement matrix and fiber, resulting in a higher modulus of rupture. Gencil et al. [16] reported an increase in flexural strength at 18 days by 6%, 11%, and 88% for basalt-fiber concrete containing 1%, 2%, and 3% fiber, respectively, with the replacement of 15% cement with silica fume. At an earlier age, i.e., 7 days, they recorded a higher increment in flexural strengths. Similarly, Saradar, Nemati [37] and Sadrumontazi, et al. [17] reported a comparable improvement in flexural strength in natural-fiber-reinforced concrete when silica fume was used as a partial substitute to cement. On the contrary, when a higher content of silica fume (15%) was used, it decreased the flexural strength. This might be due to the larger surface area of silica fume, making it absorb more water. This significantly reduced the consistency of the fresh concrete and resulted in poor compaction, packing and fiber distribution within the cement matrix, leading to increased porosity and discontinuities within the microstructure, causing premature failure to occur and consequently lowering flexural strength.

### 3.4. Splitting Tensile Strength

The results of the splitting tensile strength of the DPF-reinforced concrete are presented in Figure 10. Adding up to 2% DPF improved the tensile strength of the concrete. This was noticed as the splitting tensile strength of M1F0S was higher than that of the control by 5.3%, 8.9%, and 12.6% at 3, 7, and 28 days, respectively. The tensile strength of M2F0S was superior by 11.4% and 16.5% at 7 and 28 days, respectively, compared to the control. This enhancement in the tensile strength was ascribed to the crack arrest through the fiber-bridging effect and fiber transfer energy. This resulted in an increased post-cracking load resistance and a higher tensile strength [45]. Other fibers such as jute, sisal, coconut, and sugarcane fibers were found to increase the tensile strength of concrete, as testified by Jamshaid, Mishra [46]. However, the addition of 3% DPF decreased the tensile strength of the composite, whereas for M3F0S the strength was less than the control by 15%, 7.2%, and 14.6% at 3, 7, and 28 days, respectively. This might be due to poor dispersion and the balling effect of the fiber, which, in addition to air being entrapped during mixing on the fiber surface, resulted in an increased porosity in the cement matrix. This caused a weak and discontinuous path leading to premature failure upon load application, thus causing a reduction in the tensile strength. Another reason might be ascribed to lack of proper adhesion between the DPF and cement matrix. The inclusion of silica fume resulted in a further enhancement in the splitting tensile strength of the concrete. The replacement of 5% and 10% cement with silica fume successfully mitigated the undesirable effects of the addition of 3% DPF on the tensile strength of the DPF-reinforced concrete. This can be explained by comparing the tensile strength values of mixes M3F5S and M3F10S with that of the control. For mix M3F5S, its tensile strength was greater at 3, 7, and 28 days by 18.9%, 21.5%, and 11.3%, respectively, compared to the control. Similarly, the tensile strength of M3F10S at 3, 7, and 28 days were greater by 14.6%, 21.1%, and 15.4%, respectively, compared to the control. Additionally, even for the mixes containing 1% and 2% DPF, adding silica fume further increased their tensile strengths. Saradar, Nemati [37] reported an increase in tensile strength by 10% with the replacement of 10% cement with silica fume in basalt-fiber-reinforced concrete made with up to 0.5% fiber, while Fallah and

Nematzadeh [47] recorded an improvement in tensile strength by 17.33%, 28.37%, and 25.17% with the replacement of 8%, 10%, and 12% cement with silica fume, respectively, in polypropylene-fiber-reinforced concrete. They attributed the increment to the enhancement of bonding between the cement matrix and fiber/aggregate. The improvement in the tensile strength of the DPF concrete with the addition of silica fume was due to the microstructural and fiber/aggregate–paste bond enhancement and the resulting filler effect and reactivity of the silica fume [44]. On the contrary, the substitution of 15% cement with silica fume also decreased the splitting tensile strength of the DPF-reinforced concrete containing any percentage of fiber addition. The reason for such a decrease was the same as compressive strength results.

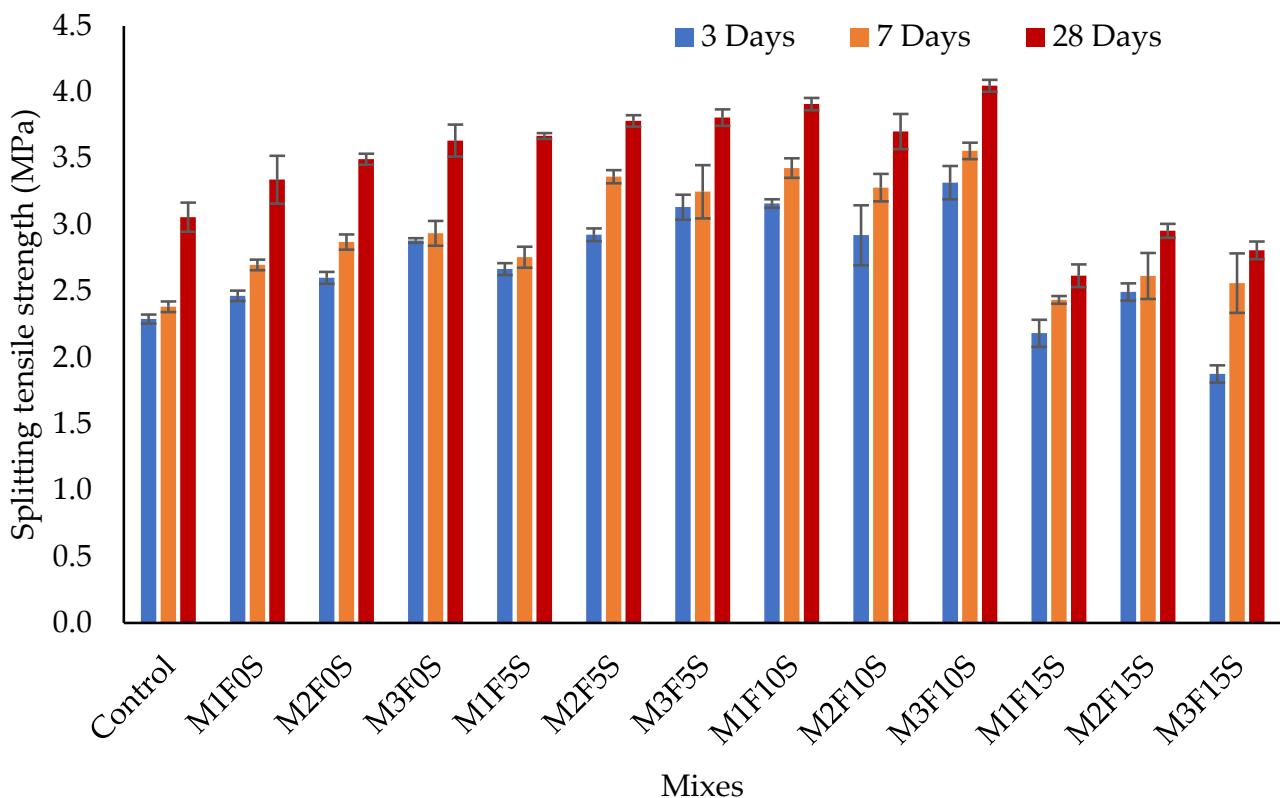


**Figure 10.** Splitting tensile strength results.

### 3.5. Water Absorption

The rate of water absorption is one of the methods of measuring porosity, which is a measuring factor influencing concrete's durability. The results of the water absorption for the DPF-reinforced concrete are presented in Figure 11. The water absorption was found to increase with the increment in the percentage addition of DPF. The water absorption for mixes M1F0S, M2F0S, and M3F0S was greater than the control by 4.9%, 21%, and 30.5%, respectively. The surge in water absorption was ascribed to the fiber's ligno-cellulose nature, making it hydrophilic and hence absorbing more water when mixing. This increased the porosity in the hardened cement matrix after drying, resulting in higher water absorption. Additionally, DPF can absorb water by up to 300% of its dry mass during mixing or curing, which can easily swell and promote micro-crack formation in the cement matrix, thereby causing a higher rate of water absorption [11,48]. A similar escalation in water absorption with the incorporation of DPF to the cement composite was reported by Bamaga [49] where they reported an increase of 27% and 74% with the inclusion of 1% and 3% DPF, correspondingly. However, the increase in water absorption for this study was lower compared to previous findings; this was due to the treatment of the fiber using NaOH solution, which significantly reduced the lignin and hemicellulose content of the fiber and

created hydrophobicity in the fiber [10]. This resulted in a decline in the rate of water absorption in the concrete. Similar findings were reported by Ozerkan, Ahsan [10] where they found that the alkaline treatment of DPF removed hemicellulose and lignin from its surface and hence led to a reduction in the water absorption of the composite when the alkaline-treated DPF was added. The partial substitution of cement with silica fume caused a decline in the water absorption of the concrete. For the mixes containing 5% silica fume, the water absorption values of the concrete with 1% and 2% DPF were lesser than that of the control by 7.1% and 2.9%, respectively. Similarly, for the mixes containing 10% silica fume, their water absorptions of the concrete with 1%, 2%, and 3% were less by about 21.1%, 16.5%, and 6.1%, respectively, compared to the control mix. Similar findings were reported by Saradar, Nemati [37] where they reported a decline in water absorption by up to 38% with the replacement of 10% cement using silica fume in basalt-fiber-reinforced concrete containing up to 0.5% fiber, while Fallah and Nematzadeh [47] reported a reduction in water absorption by 18% with the replacement of 12% cement with silica fume in polypropylene-fiber reinforced composite. The decline in water absorption by the inclusion of silica fume in the DPF composite resulted from the lower porosity due to the formation of excess hydration products. The generated hydration products densified the pores generated by the DPF in the matrix and hence refined the microstructure of the DPF-reinforced concrete yielding a lower water absorption [44]. However, 15% silica content in the DPF composite caused an increase in water absorption, which became more severe with the increment in the addition of DPF. This might be due to the fineness of silica fume, which caused further absorption of mixing water, thereby reducing the consistency of the paste. This caused poor compaction and distribution of the fibers within the matrix and thus led to honeycombs and voids within the concrete microstructure and, consequently, a higher water absorption. Khan [50] also reported similar findings, where up to 10% silica fume addition as the SCM in conventional concrete decreased its water absorption, but 15% increased it.

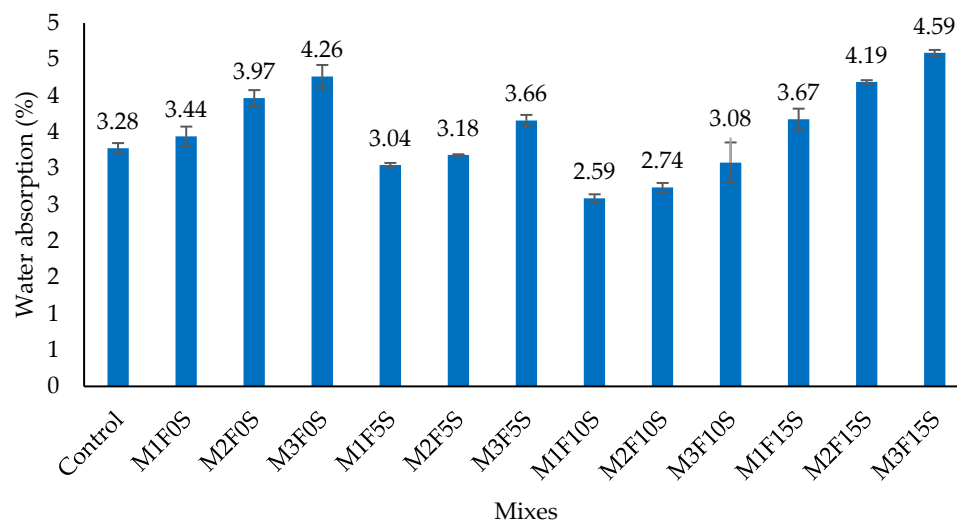


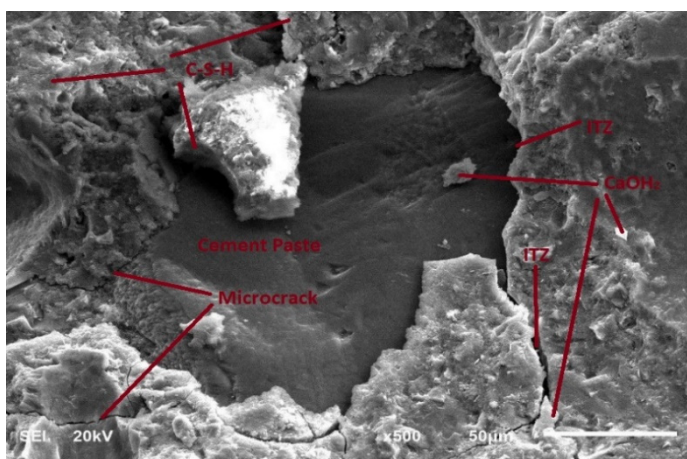
**Figure 11.** Water absorption results.

### 3.6. FESEM Analysis

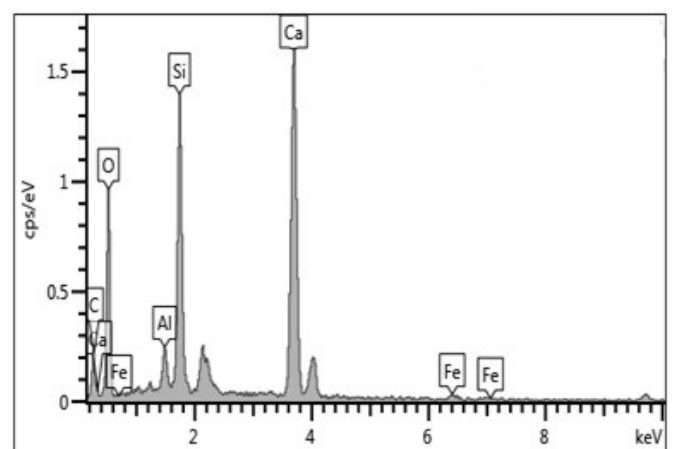
FESEM analysis was used to obtain and study the microstructural morphology of some of the representative mixes of the DPF-reinforced concrete, where the effects of DPF addition and the partial replacement of cement with silica fume were analyzed. Figure 12a–e presents the morphology of some selected DPF concrete mixes. From the morphology of the control mix in Figure 12a, traces of  $\text{Ca}(\text{OH})_2$  and C-S-H were seen resulting from the cement hydration reaction. Additionally, some micro-cracks might have resulted from plastic or drying shrinkage. Furthermore, the interfacial transition zone (ITZ) between the cement paste and aggregate could be seen and was densified by the hydration products. For all other mixes containing DPF, i.e., Figure 12b–e, DPF could be seen on the

microstructure, without been disintegrated due to applied loads. Around the surface of the DPF, traces of hydration compounds such as C-S-H and  $\text{Ca}(\text{OH})_2$  were also seen to be deposited on the fiber surfaces. Furthermore, it was observed that the ITZ between the DPF and cement matrix was porous, which was attributed to poor bonding between the cement matrix and the fiber. For example, considering Figure 12e, i.e., the morphology of M2F0S, its ITZ was the most porous, resulting in poor adhesion between the fiber and cement matrix. Furthermore, the hydrophilic nature of the DPF due to the presence of ligno-cellulose compounds increased the voids in the matrix through the absorption of more water and entrapment of air during mixing, which eventually dried up, leaving pores in the matrix [11,48]. This, consequently, is one of the reasons for the diminution in the mechanical strength and durability of the concrete with the inclusion of DPF. Similar results have been established by Kriker, Debicki [42]. Partial cement replacement with silica fume densified the microstructure and ITZ between the DPF and cement paste. The mixture containing 1% DPF and 10% silica fume in Figure 12c had the most densified microstructure, with the ITZ being filled and densified with the cement hydration and silica fume pozzolanic reaction products. This densification enhanced the bonding between the fiber and cement paste as displayed in Figure 12c. The improvement was ascribed to the reaction between  $\text{SiO}_2$  from silica fume with  $\text{CaOH}_2$  from cement hydration. This led to surplus C-S-H generation, which densified the concrete's ITZ and microstructure. Additionally, the consumption of  $\text{CaOH}_2$  also decreased its leaching out with time, reducing the pore generation caused by the leachate.

Energy dispersive X-ray (EDX) analysis was used to obtain and analyze the elemental configurations of some of the randomly selected DPF-reinforced concrete containing silica fume. The results are summarized in Table 4 and Figure 12i–v. The main elements present in all the cement matrices included silicon (Si), carbon (C), calcium (Ca), aluminum (Al), oxygen ( $\text{O}_2$ ), and iron (Fe). Other traces of elements and impurities in minor form were also present. Mixes containing silica fume such as M1F1S (Figure 12ii), M1F10S (Figure 12iii), and M1F15S (Figure 12iv) had abundant Si and  $\text{O}_2$  with less Ca. This explained or indicated that pozzolanic reactions took place between the  $\text{SiO}_2$  from the silica fume and  $\text{Ca}(\text{OH})_2$  from the cement to produce excess C-S-H [51]. This can be elaborated more by comparing their ratios of Ca/Si and Si/Al with the other mixes. It can be observed from Table 4 that the mix M1F10S had the smallest value of Ca/Si and the greatest value of Si/Al, which signified the highest pozzolanic reaction, while mix M2F0S had the greatest value of Ca/Si and smallest value of Si/Al, thus denoting the least pozzolanic reaction due to the non-presence of silica fume.



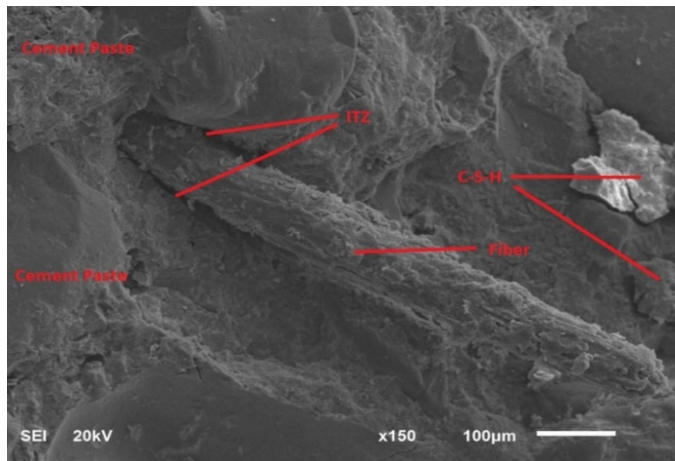
(a) FESEM of control mix



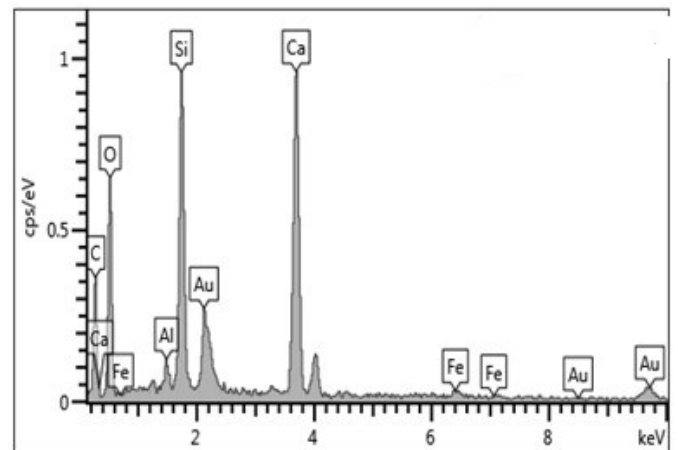
(i) EDX of control mix

Figure 12. Cont.

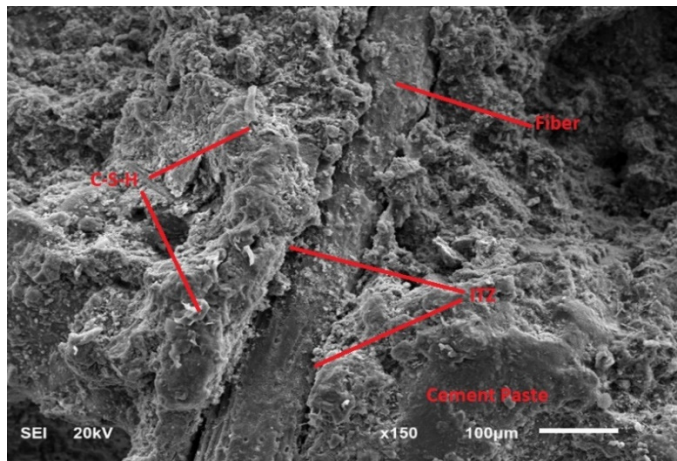




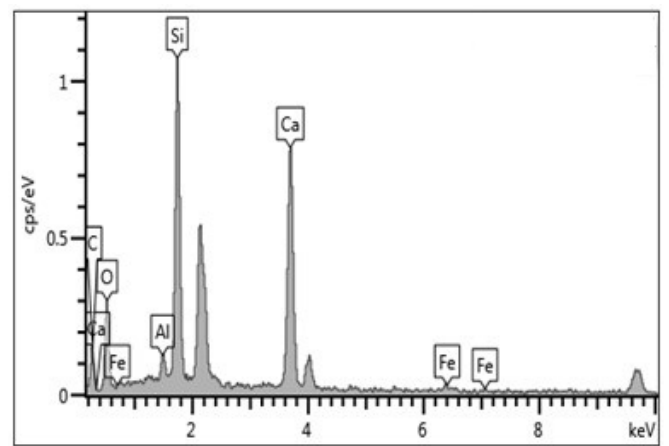
(b) FESEM of mix M1F5S



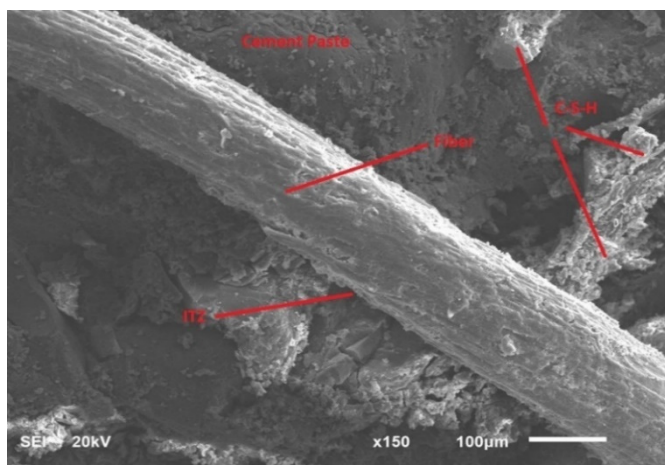
(ii) EDX of mix M1F5S



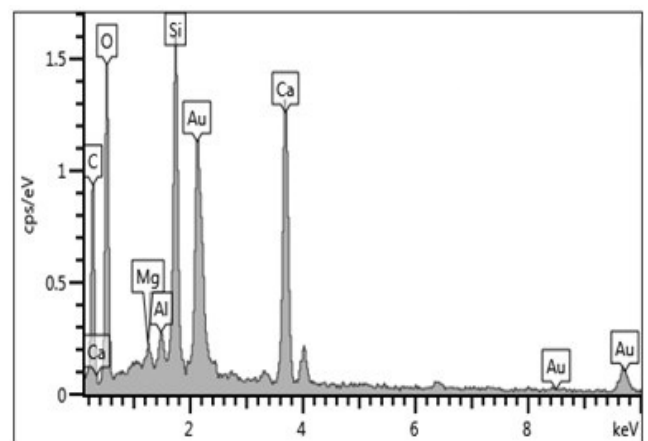
(c) FESEM of mix M1F10S



(iii) EDX of mix M1F10S



(d) FESEM of mix M1F15S



(iv) EDX of mix M1F15S

Figure 12. Cont.

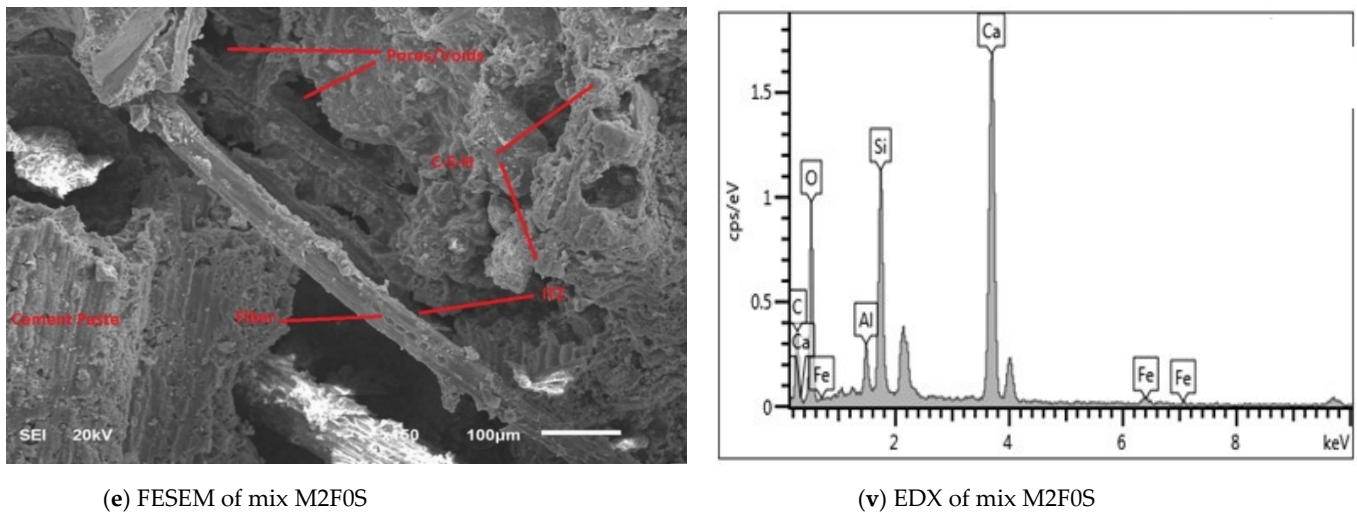


Figure 12. Microstructural morphology of DPF-reinforced concrete.

Table 4. Elemental compositions obtained from EDX analysis.

Elements	Atomic Weight Concentration (%)				
	Control	M2F0S	M1F10S	M1F5S	M1F15S
C	18.15	23.91	28.87	31.61	37.01
O	48.98	46.01	33.84	43.38	44.73
Al	1.55	1.73	1.35	0.79	0.75
Si	9.63	7.04	14.4	8.08	6.49
Ca	20.98	20.22	20.6	15.32	10.52
Fe	0.71	1.09	0.95	0.82	-
Mg	-	-	-	-	0.5
Total	100	100	100	100	100
Si/Al	6.21	4.07	10.67	10.23	8.65
Ca/Si	2.18	2.87	1.43	1.90	1.62
Ca/(Si + Al)	1.88	2.31	1.31	1.73	1.45

#### 4. Conclusions

This study investigated the effects of silica fume as an SCM on the mechanical properties of DPF-reinforced concrete. Some of the conclusions summarized include:

- (1) The fresh and hardened densities of the DPF-reinforced concrete declined with the addition of DPF by weight of binder materials and partial substitution of cement with silica fume.
- (2) The compressive strength of the DPF-reinforced concrete declined with the increase in DPF content as an additive by weight of binder materials.
- (3) The incorporation of up to 2% DPF by weight of binder constituents enhanced the splitting tensile and flexural strengths of the DPF-reinforced concrete.
- (4) The addition of DPF increased the porosity of the DPF-reinforced concrete as measured through the increment in water absorption with the addition of DPF.
- (5) Partially substituting cement with silica fume significantly enhanced the mechanical strength of the DPF-reinforced concrete. The loss in compressive strength up to 2% DPF addition was mitigated by replacing up to 10% cement with silica fume.
- (6) Silica fume densified the microstructure and refined the ITZ between the fiber and cement matrix, hence significantly reducing the porosity and enhancing the durability.
- (7) A sustainable DPF-reinforced concrete mix was produced by adding up to 2% DPF by weight of binder materials and replacing up to 10% cement with silica fume.

**Author Contributions:** Conceptualization, Y.E.I. and M.A.; methodology, M.A., M.L.M., O.S.A. and Q.A.D.; software M.A. and M.L.M.; validation, M.A., Y.E.I. and M.A.M.; formal analysis, M.A. and Q.A.D.; investigation, Y.E.I., M.A., M.L.M. and M.A.M.; resources, O.S.A. and M.A.M.; data curation, M.A. and M.L.M.; writing—original draft preparation, M.A. and M.L.M.; writing—review and editing, Y.E.I. and M.A.M.; visualization, O.S.A. and M.A.M.; supervision, Y.E.I.; project administration, Y.E.I. and O.S.A.; funding acquisition, Y.E.I. All authors have read and agreed to the published version of the manuscript.

**Funding:** This research was supported by the Structures and Materials (S&M) Research Laboratory of Prince Sultan University, Saudi Arabia. Furthermore, the authors acknowledge the support of Prince Sultan University in paying the article processing charges (APC) of this publication.

**Data Availability Statement:** Not applicable.

**Acknowledgments:** The authors wish to acknowledge the support of the Structures and Materials laboratory (S&M Lab) of the College of Engineering, Prince Sultan University, Riyadh, Saudi Arabia, for their vital support.

**Conflicts of Interest:** The authors declare no conflict of interest.

## References

- Vantadori, S.; Carpinteri, A.; Zanichelli, A. Lightweight construction materials: Mortar reinforced with date-palm mesh fibres. *Theor. Appl. Fract. Mech.* **2019**, *100*, 39–45. [[CrossRef](#)]
- Yousefi, M.; Khandestani, R.; Gharaei-Moghaddam, N. Flexural behavior of reinforced concrete beams made of normal and polypropylene fiber-reinforced concrete containing date palm leaf ash. *Structures* **2022**, *37*, 1053–1068. [[CrossRef](#)]
- Zhang, P.; Han, S.; Golewski, G.L.; Wang, X. *Nanoparticle-Reinforced Building Materials with Applications in Civil Engineering*; SAGE Publications Sage UK: London, UK, 2020; p. 1687814020965438.
- Bentur, A.; Mindess, S. *Fibre Reinforced Cementitious Composites*; CRC Press: Boca Raton, FL, USA, 2006.
- Balea, A.; Fuente, E.; Monte, M.C.; Blanco, Á.; Negro, C. Fiber reinforced cement based composites. In *Fiber Reinforced Composites*; Elsevier: Amsterdam, The Netherlands, 2021; pp. 597–648.
- Balaguru, P.N.; Shah, S.P. *Fiber-Reinforced Cement Composites*; McGraw-Hill: New York, NY, USA, 1992.
- Banthia, N. Fiber reinforced concrete. In *ACI SP-142 Fiber Reinforced Concrete Developments and Innovations*; American Concrete Institute: Farmington Hills, MI, USA, 1994; Volume 91, p. 119.
- Banthia, N. *ACI 544.5R-Report on the Physical Properties and Durability of Fiber-Reinforced Concrete*; American Concrete Institute: Farmington Hills, MI, USA, 2010.
- Al-Oqla, F.M.; Allothman, O.Y.; Jawaid, M.; Sapuan, S.M.; Es-Saheb, M.H. Processing and Properties of Date Palm Fibers and its Composites. In *Biomass and Bioenergy*; Springer: Berlin/Heidelberg, Germany, 2014; pp. 1–25.
- Ozerkan, N.G.; Ahsan, B.; Mansour, S.; Iyengar, S. Mechanical performance and durability of treated palm fiber reinforced mortars. *Int. J. Sustain. Built Environ.* **2013**, *2*, 131–142. [[CrossRef](#)]
- Benaniba, S.; Driss, Z.; Djendel, M.; Raouache, E.; Boubaaya, R. Thermo-mechanical characterization of a bio-composite mortar reinforced with date palm fiber. *J. Eng. Fibers Fabr.* **2020**, *15*, 1558925020948234. [[CrossRef](#)]
- Zanichelli, A.; Carpinteri, A.; Fortese, G.; Ronchei, C.; Scorza, D.; Vantadori, S. Contribution of date-palm fibres reinforcement to mortar fracture toughness. *Procedia Struct. Integr.* **2018**, *13*, 542–547. [[CrossRef](#)]
- Kareche, A.; Agoudjil, B.; Haba, B.; Boudenne, A. Study on the Durability of New Construction Materials Based on Mortar Reinforced with Date Palm Fibers Wastes. *Waste Biomass Valorization* **2020**, *11*, 3801–3809. [[CrossRef](#)]
- Alatshan, F.; Altlomite, A.M.; Mashiri, F.; Alamin, W. Effect of date palm fibers on the mechanical properties of concrete. *Int. J. Sustain. Build. Technol. Urban Dev.* **2017**, *8*, 68–80.
- Hakkoum, S.; Kriker, A.; Mekhermeche, A. Thermal characteristics of Model houses Manufactured by date palm fiber reinforced earth bricks in desert regions of Ouargla Algeria. *Energy Procedia* **2017**, *119*, 662–669. [[CrossRef](#)]
- Bamaga, S.O. A Review on the Utilization of Date Palm Fibers as Inclusion in Concrete and Mortar. *Fibers* **2022**, *10*, 35. [[CrossRef](#)]
- Adamu, M.; Alanazi, F.; Ibrahim, Y.E.; Alanazi, H.; Khed, V.C. A Comprehensive Review on Sustainable Natural Fiber in Cementitious Composites: The Date Palm Fiber Case. *Sustainability* **2022**, *14*, 6691. [[CrossRef](#)]
- Alawar, A.; Hamed, A.M.; Al-Kaabi, K. Characterization of treated date palm tree fiber as composite reinforcement. *Compos. Part B Eng.* **2009**, *40*, 601–606. [[CrossRef](#)]
- Wazzan, A.A. Effect of fiber orientation on the mechanical properties and fracture characteristics of date palm fiber reinforced composites. *Int. J. Polym. Mater. Polym. Biomater.* **2005**, *54*, 213–225. [[CrossRef](#)]
- Gencil, O.; Nodehi, M.; Bayraktar, O.Y.; Kaplan, G.; Benli, A.; Gholampour, A.; Ozbakkaloglu, T. Basalt fiber-reinforced foam concrete containing silica fume: An experimental study. *Constr. Build. Mater.* **2022**, *326*, 126861. [[CrossRef](#)]
- Sadrmomtazi, A.; Tahmouresi, B.; Saradar, A. Effects of silica fume on mechanical strength and microstructure of basalt fiber reinforced cementitious composites (BFRCC). *Constr. Build. Mater.* **2018**, *162*, 321–333. [[CrossRef](#)]

22. Khan, M.; Rehman, A.; Ali, M. Efficiency of silica-fume content in plain and natural fiber reinforced concrete for concrete road. *Constr. Build. Mater.* **2020**, *244*, 118382. [[CrossRef](#)]
23. Zhang, P.; Wang, K.; Wang, J.; Guo, J.; Hu, S.; Ling, Y. Mechanical properties and prediction of fracture parameters of geopolymer/alkali-activated mortar modified with PVA fiber and nano-SiO<sub>2</sub>. *Ceram. Int.* **2020**, *46*, 20027–20037. [[CrossRef](#)]
24. Golewski, G. Green Concrete Based on Quaternary Binders with Significant Reduced of CO<sub>2</sub> Emissions. *Energies* **2021**, *14*, 4558. [[CrossRef](#)]
25. Golewski, G.L. An extensive investigations on fracture parameters of concretes based on quaternary binders (QBC) by means of the DIC technique. *Constr. Build. Mater.* **2022**, *351*, 128823. [[CrossRef](#)]
26. Gil, D.M.; Golewski, G.L. Potential of siliceous fly ash and silica fume as a substitute for binder in cementitious concretes. *E3S Web Conf.* **2018**, *49*, 00030. [[CrossRef](#)]
27. *ASTM C150/150M*; Standard Specification for Portland Cement. ASTM International: West Conshohocken, PA, USA, 2015.
28. *ASTM C33*; Standard Specification for Concrete Aggregates. ASTM International: West Conshohocken, PA, USA, 2018.
29. Ali-Boucetta, T.; Ayat, A.; Laifa, W.; Behim, M. Treatment of date palm fibres mesh: Influence on the rheological and mechanical properties of fibre-cement composites. *Constr. Build. Mater.* **2021**, *273*, 121056. [[CrossRef](#)]
30. *ACI 211.1R*; Standard Practice for Selecting Proportions for Normal, Heavyweight, and Mass Concrete. American Concrete Institute: Farmington Hills, MI, USA, 2002.
31. *BS-EN 12350-6*; Testing Fresh Concrete. Density. British Standard Institution: London, UK, 2019.
32. *BS EN 12390-7*; Testing Hardened Concrete. Density of Hardened Concrete. British Standards Institution: London, UK, 2019.
33. *BS EN 12390-3*; Testing Hardened Concrete. Compressive Strength of Test Specimens. British Standards Institution: London, UK, 2009.
34. *ASTM C78/C78M*; Standard Test Method for Flexural Strength of Concrete (Using Simple Beam with Third-Point Loading). ASTM International: West Conshohocken, PA, USA, 2015.
35. *ASTM C642*; Standard Test Method for Density, Absorption, and Voids in Hardened Concrete. ASTM International: West Conshohocken, PA, USA, 2001.
36. Rachedi, M.; Kriker, A. Thermal Properties of Plaster Reinforced with Date Palm Fibers. *Civ. Environ. Eng.* **2020**, *16*, 259–266. [[CrossRef](#)]
37. Saradar, A.; Nemati, P.; Paskiabi, A.S.; Moein, M.M.; Moez, H.; Vishki, E.H. Prediction of mechanical properties of lightweight basalt fiber reinforced concrete containing silica fume and fly ash: Experimental and numerical assessment. *J. Build. Eng.* **2020**, *32*, 101732. [[CrossRef](#)]
38. Boumhaout, M.; Boukhattem, L.; Hamdi, H.; Benhamou, B.; Nouh, F.A. Thermomechanical characterization of a bio-composite building material: Mortar reinforced with date palm fibers mesh. *Constr. Build. Mater.* **2017**, *135*, 241–250. [[CrossRef](#)]
39. Pickering, K.L.; Aruan Efendy, M.G.; Le, T.M. A review of recent developments in natural fibre composites and their mechanical performance. *Compos. Part A Appl. Sci. Manuf.* **2016**, *83*, 98–112. [[CrossRef](#)]
40. Kriker, A.; Bali, A.; Debicki, G.; Bouziane, M.; Chabannet, M. Durability of date palm fibres and their use as reinforcement in hot dry climates. *Cem. Concr. Compos.* **2008**, *30*, 639–648. [[CrossRef](#)]
41. Benaimeche, O.; Carpinteri, A.; Mellas, M.; Ronchei, C.; Scorza, D.; Vantadori, S. The influence of date palm mesh fibre reinforcement on flexural and fracture behaviour of a cement-based mortar. *Compos. Part B Eng.* **2018**, *152*, 292–299. [[CrossRef](#)]
42. Kriker, A.; Debicki, G.; Bali, A.; Khenfer, M.; Chabannet, M. Mechanical properties of date palm fibres and concrete reinforced with date palm fibres in hot-dry climate. *Cem. Concr. Compos.* **2005**, *27*, 554–564. [[CrossRef](#)]
43. Nochaiya, T.; Wongkeo, W.; Chaipanich, A. Utilization of fly ash with silica fume and properties of Portland cement–fly ash–silica fume concrete. *Fuel* **2010**, *89*, 768–774. [[CrossRef](#)]
44. Siddique, R. Utilization of silica fume in concrete: Review of hardened properties. *Resour. Conserv. Recycl.* **2011**, *55*, 923–932. [[CrossRef](#)]
45. Abbass, W.; Khan, M.I.; Mourad, S. Evaluation of mechanical properties of steel fiber reinforced concrete with different strengths of concrete. *Constr. Build. Mater.* **2018**, *168*, 556–569. [[CrossRef](#)]
46. Jamshaid, H.; Mishra, R.K.; Raza, A.; Hussain, U.; Rahman, L.; Nazari, S.; Chandan, V.; Muller, M.; Choteborsky, R. Natural Cellulosic Fiber Reinforced Concrete: Influence of Fiber Type and Loading Percentage on Mechanical and Water Absorption Performance. *Materials* **2022**, *15*, 874. [[CrossRef](#)] [[PubMed](#)]
47. Fallah, S.; Nematzadeh, M. Mechanical properties and durability of high-strength concrete containing macro-polymeric and polypropylene fibers with nano-silica and silica fume. *Constr. Build. Mater.* **2017**, *132*, 170–187. [[CrossRef](#)]
48. Benmansour, N.; Agoudjil, B.; Gherabli, A.; Kareche, A.; Boudenne, A. Thermal and mechanical performance of natural mortar reinforced with date palm fibers for use as insulating materials in building. *Energy Build.* **2014**, *81*, 98–104. [[CrossRef](#)]
49. Bamaga, O.S. Physical and mechanical properties of mortars containing date palm fibers. *Mater. Res. Express* **2022**, *9*, 015102. [[CrossRef](#)]
50. Khan, M. Isoresponses for strength, permeability and porosity of high performance mortar. *Build. Environ.* **2003**, *38*, 1051–1056. [[CrossRef](#)]
51. Kelechi, S.E.; Uche, O.A.U.; Adamu, M.; Alanazi, H.; Okokpujie, I.P.; Ibrahim, Y.E.; Obianyo, I.I. Modeling and Optimization of High-Volume Fly Ash Self-Compacting Concrete Containing Crumb Rubber and Calcium Carbide Residue Using Response Surface Methodology. *Arab. J. Sci. Eng.* **2022**, 1–20. [[CrossRef](#)]